RSC Advances

ROYAL SOCIETY OF CHEMISTRY

www.rsc.org/advances

Analysis of Moisture Diffusion Mechanism in Structured Lipids using Magnetic Resonance Imaging

Sravanti Paluri,[a] Mohammed Shavezipur,[a] Dennis R. Heldman, [a,b] and Fatemeh Maleky[b,*]

[a] Department of Food, Agricultural and Biological Engineering, The Ohio State University, Columbus, OH, USA.

[b] Department of Food Science and Technology, The Ohio State University, Columbus, OH, USA.

*Corresponding author email: maleky.1@osu.edu

Abstract

The mechanism of moisture migration from a high water-content gel-layer to an adjacent lipid layer was characterized. Three lipid samples: cocoa butter (CB), palm kernel oil (PO) and 20% (w/w) cocoa powder in palm kernel oil (CPPO) were prepared by two methods, shearing during crystallization and static crystallization. Using Magnetic Resonance Imaging, samples' moisture uptake at a storage temperature of 20 ºC was measured for 91 days and their effective diffusivity values were calculated. It was found that shearing reduces effective diffusivity of moisture in samples, thereby increasing their moisture-barrier capacity compared to unprocessed lipid systems. The mechanism of moisture migration was found to be a combination of Fickian diffusion and relaxation of lipid matrix in the statically crystallized cocoa butter samples, whereas Fickian diffusion was the dominant mechanism in sheared cocoa butter samples. Palm kernel oil samples exhibited a combination of Fickian and relaxation mechanisms, regardless of the processing technique. Whereas the mixture of palm kernel oil and cocoa powder samples showed relaxation-mechanism controlled migration due to the presence of hydrophilic cocoa powder particles.

Main Text

Moisture transfer occurs between a food and its environment or between two layers in a multicomponent food due to the existence of a water activity gradient[1-3]. In such systems, movement of moisture from higher to lower water activity layer occurs until a thermodynamic equilibrium state is achieved[4,5]. Problems caused due to such an increase in moisture content during storage include microbial growth and undesirable changes in taste, appearance and texture. Several solutions have been proposed to reduce moisture transfer, such as, improving process or storage parameters, changing product formulation to reduce water activity gradients and use of non-edible or edible films as moisture barriers[1]. It may not be always possible to implement changes in storage parameters or formulations without affecting sensory characteristics of the food product. Moreover, usage of non-edible barriers is also not a feasible application in most food products[1]. Therefore, edible barriers based on hydrophobic materials, such as lipids, have been developed for specific use as moisture barriers in foods[3,6]. Lipid components and lipid-based films have been successfully used to limit moisture migration in candies, confectioneries, frozen baked goods and frozen desserts[7]. For example, chocolate coating on the inside of an ice cream cone is used to maintain crispness of the cone wafer during storage. Cocoa butter, as the main lipid component of chocolate, is responsible for reducing moisture transfer from filling to cone.

The water vapor permeability (WVP) of lipid films has been shown to depend on the film composition, physical state of ingredients, crystalline structure, thermodynamics and physical state of water in contact[6,8,9,10]. Among these factors, structural properties such as apparent domain size, crystalline arrangement, crystal sizes and/or distribution have a strong influence on WVP[3]. A number of studies introduce the application of external forces, such as shearing, as an

effective tool to change the structural properties of lipids during the crystallization process[11-14]. Shearing produces smaller crystal sizes due to reduced interlocking and agglomeration in crystals[15]. A strong effect of changing lipid structure by processing is observed in the case of oil migration in cocoa butter[16,17]. Similarly, structure at the scale of fat crystal network as well as within the crystal is also expected to have an effect on moisture migration[18]. In edible films, WVP has been shown to decrease with lipid particle size[19,20].

In order to measure moisture migration in various lipid systems, different techniques have been used in the past. A gravimetric technique (using original or modified ASTM method E 96-95) has been extensively used to evaluate WVP in various edible films[20-22]. However, Ghosh et al. identified some drawbacks of this method, such as improper film support, difficulty in sealing, inaccurate determination of exact vapor pressure differences across the film[18]. Aside from drawbacks in methodology, Watanabe and Fukuoka compared measurement of moisture diffusion coefficient in soybean by gravimetric and another technique known as pulsed field gradient (PFG) nuclear magnetic resonance (NMR)[23]. Their work reported two limitations of measuring diffusivity through gravimetric technique, (i) measurement of apparent diffusivity of water averaged over different components of soybean such as cell membrane, epidermis, vacuoles, which may have different rates of diffusion, and, (ii) it was also based on assumptions related to instantaneous equilibrium at the surface, spherical shape of cells, volume changes etc. Due to these limitations, Watanabe and Fukuoka suggested PFG NMR as a better technique to measure intrinsic diffusivity without any of the assumptions made in gravimetric technique. Although accurate, PFG NMR can only measure the self-diffusion which is not always practical since most food products are not homogenous[18]. Besides these analytical methods, magnetic resonance imaging (MRI) was introduced as a powerful tool which has the potential to better

investigate moisture uptake and migration into low moisture content foods[24]. MRI measures mutual-diffusion coefficients (effective diffusivity) in more realistic heterogeneous food systems, and has therefore been used recently to measure oil and moisture migration in foods. For instance, it was used to study oil migration in chocolate[25] and in chocolate-peanut butter paste confectionary[26]. Other studies investigated the presence of moisture in foods using MRI, for example, Lodi et al. characterized water distribution in bread during storage[27], and Troutman et al. observed moisture migration in soft-panned confections[28].

Although much work has been done on determination of WVP and effect of structure on WVP of lipid films, a better understanding of liquid-phase water migration in lipids is needed. An explanation of the mechanism of moisture migration will be useful for making lipid-based moisture barriers, such as lipid laminates and emulsions. This study aims to examine the effect of processing conditions on effective diffusivity and the mechanism of moisture transport using well known principles of mass transfer. Using MRI as one of the advanced techniques, water uptake from a gel-water source through a crystalline fat matrix will be measured. For this purpose, three lipid samples; cocoa butter, palm kernel oil, and 20% w/w cocoa powder in palm kernel oil are prepared with two processing techniques: application of an external force during crystallization and static crystallization. Water migration data along with Fick's II Law of Diffusion will be used to determine effective diffusivity values and examine the effect of processing. Experimental data will also be used to characterize the mechanism of moisture migration into processed and non-processed lipids.

The cocoa butter used in this study was donated by Mars Chocolate North America (Hackettstown, New Jersey, USA). Palm kernel oil was provided by IOI Group Loders Croklaan (Illinois, USA). Canola oil and Hershey's cocoa powder were purchased at a nearby

supermarket. Granulated Agar powder (microbiology grade BD Difco Dehydrated Culture Media, New Jersey, USA) was used to prepare the gel source for water.

Lipid samples were prepared in triplicates by two processes; static and dynamic crystallization. The lipid was heated at 60 ºC to ensure complete melting and held at that temperature for 20-25 minutes to destroy all crystal memory. For static sample, the molten lipid sample at 60 ºC was poured into a mold (3 cm length by 3 cm width by 3 cm height) and immediately transferred to 20 ºC storage for 1 day to complete crystallization. Sheared sample was prepared by using a stirrer (Model BDC3030, Caframo Limited, Wiarton, Ontario, Canada) with a pitched 3-bladed propeller agitating the melt at 250 s^{-1}. While shearing, cooling was achieved by submerging the stirring assembly in a water bath manually maintained at 20 ºC. The mixture was stirred continuously for about 15 min. The partially crystallized sample was transferred into a mold (3 cm length by 3 cm width by 3 cm height). All molds containing static and sheared lipid samples were stored at 20 ºC for 1 day to complete the crystallization.

The gel-water layer was prepared by dissolving 1.5g agar powder in 98.5g water. This mixture was heated at 80 ºC until the powder dissolved. Hot agar solution was poured into vials (clear Amac plastic container, The Container Store, Ohio, USA) of dimensions 6 cm in height and with 3 cm by 3 cm square base; until they were approximately half-full. The vial was cooled to ensure complete gelation and equilibrated to experimental condition (20 ºC) for one day. To prepare the two-layered samples, crystallized lipid samples were taken out of the molds, flattened manually and inverted into the vial to put in contact with the gel layer. Care was taken to maintain the lipid-gel interface as flat as possible. The vial was hermetically sealed with para-film and cellophane tape. Triplicates of these two-layered samples were stored for three months at 20 ºC during which moisture migration was periodically measured using MRI equipment

operating at the same temperature. Henceforth the following short-hand will be used to identify the samples: CB for cocoa butter, PO for palm kernel oil, CPPO for 20% w/w cocoa powder in palm kernel oil. A control vial with time-invariant canola oil was prepared as a monolayer sample and imaged in MRI along with the samples.

Solid fat content (SFC) of samples was measured prior to starting the MRI experiment by means of pulsed nuclear magnetic resonance (p-NMR). Glass NMR tubes (10 mm diameter, 1 mm thickness, and 180 mm height) were filled with approximately 3 g of crystallized samples that had been cut in smaller pieces. Using Bruker Minispec spectrometer (Bruker Optics Ltd., ON, Canada), the amount of solid particles were calculated and reported in Table 1. The reported data correspond to average of three individual measurements.

MR Imaging was performed on a 7 T human preclinical magnet (Achieva, Philips, Cleveland, Ohio) with an RF transmit coil that typically images human skull. The field of view of the MRI coil was 176×150 × 114 mm in which a sample mold was inserted. This mold consisted of nine samples arranged into 3 rows x 3 columns. Figure 1 (a) is a three-dimensional illustration of one of these nine samples used for MRI. The MR images were acquired using a spin echo pulse sequence with 1000 ms repetition time, 9.5 ms echo time, flip angle 90°, four averages, acquisition time 89 minutes, matrix size 768 x 768 and number of slices 57. Axial images were captured as two-dimensional slices (x and y dimension) of the mold with a resolution of 0.244 × 0.244 mm taken at every 2 mm with zero gap. Out of the total 57 slices of the mold, each sample had about 12-15 slices taken every 2 mm. Among the 12-15 slices in a sample, about seven to eleven slices with a clear interface were chosen for analysis. Next, to avoid any irregularities where the sample touched the vial walls, a central region of interest 50 mm by 50 mm in each slice was selected for further analysis. Figure 1 (b) illustrates a

representative MR image of the central region of the sample immediately after contact of the lipid and gel layers. Axes represent pixel numbers (0 to 200). The color bar represents signal intensity (SI) in arbitrary units. The agar gel meniscus has some curvature which increases towards the periphery of the sample (boundary). The signal intensity of the entire sample including the gel meniscus on the first day of measurement is taken as reference for all future tests. This reference was subtracted from all future tests so that only the change in signal intensity due to water migration in the lipid region remained. In other words, moisture uptake in lipid sample on day n is measured as the difference between the image on the first and n'th day and therefore not affected by the presence of gel meniscus on all test days. Image processing and data analysis were performed using MATLAB (R2013b, The Mathworks, Inc., Natick, MA, USA). A 1-dimensional SI profile was made by averaging SI over the width (50-150 pixels) and the noise in SI values was minimized based on a constant sum assumption of SI in the sample on each day. Acquired SI values were rotated counter-clockwise by 90^{o} and plotted as shown in Figure 1 (c). One pixel distance on an axis of the image is equivalent to 0.25 mm. The abscissa is distance in sample from lipid (0-50 pixels) to gel (50-100 pixels). The two regions are readily distinguishable by the steep gradient in SI values on either side of the interface at 50 pixels. To track the time-dependent changes in lipid layer, SI values for two days (1 and 91) of measurements were plotted on the same axis as shown in figure 1(c) to highlight changes in SI around the interface. A MATLAB program was developed to minimize sample placement error, angular tilting, and, day-to-day variation in SI values using time-invariant canola oil reference. Measurements were taken at 1, 7, 14, 20, 35, 61, 91 days of storage at 20 ºC and the same procedure was repeated for triplicates of all the samples. Moisture uptake was measured in a 2mm (8 pixels) thick region shown by two solid vertical lines in the lipid (Figure 1 (c)). Similar

to the work by Maleky et al.[17], Lee et al.[29], and Altan et al.[30], concentration of diffusing species (water) in lipid is assumed to be proportional to the difference in signal intensity at time t=t and time t=0 in the lipid phase. Amount of water uptake of the samples (M_t) was calculated by difference in area under the SI curve time t=t and time t=0 in the 8 pixel wide region of interest. Average uptake values of all samples as a function of time are plotted in Figure 2. A logarithmic trend-line was fitted to the data and shown as dotted lines for dynamic and solid lines for static samples in the figure. As seen by the trend and R^2 values indicated in the figure, for all the studied samples except dynamic CPPO, it is observed that M_t increases initially and then reaches a plateau suggesting attainment of equilibrium in these samples. This behavior of exhibiting initially high gradient in M_t followed by stabilization of gradient is typical of Fickian diffusion[22]. This stabilization of gradient can be assumed to be a pseudo steady state, which is a series of successive measurements that indicate equilibrium, M_∞[1]. In order to compare statistical differences in evolution of M_t with time of storage at 20 °C, one time point during the gradual increase (day 7) and another in the plateau region (day 91) signifying maximum uptake M_∞ were chosen. Using a student t-test conducted on JMP® Software (Cary, NC), it was found that M_t values for all samples were significantly different (p-value < 0.05) between day 7 and day 91. This comparison of M_t values for each lipid sample is presented in Figure 3 (a)-(c). Next, a statistical comparison of the equilibrium moisture uptake value between two methods of crystallization of a single type of lipid was also conducted. All samples in this study (with the exception of dynamic CPPO sample) displayed attainment of equilibrium plateau on the last three days of observation. Dynamic CPPO samples showed a marked increase on day 91 of storage which will be discussed later. Therefore as a representation of equilibrium moisture uptake, M_t values on day 61 were chosen for comparison and reported in figure 4. In this figure,

using a student t-test, it was found that all dynamically crystallized samples had significantly different M_t values from static samples ($p<0.05$). The moisture uptake M_t versus time curves in figure 2 (a)-(c) were compared for two methods of crystallization, static and dynamic using GraphPad Prism® v4.0 (La Jolla, California) which compares overall curves of two samples. It was found that for each type of lipid, CB, PO, CPPO, the M_t curves of dynamic samples were significantly different from those of static samples with p-value <0.05. To further investigate the kinetics of moisture migration in the samples, we also determined their water uptake ratios (WUR). Water uptake ratio (WUR) at any time, t, is defined as the ratio of uptake at that time (M_t) over equilibrium uptake (M_∞) and ranges from zero at initial time to one when equilibrium is achieved. Experimental WUR values of the samples over three months of storage exhibited the same trend as moisture uptake values. Using the WUR values in the original solution to Fick's second law of diffusion, effective diffusivities of samples for the given boundary condition were estimated[31]. The 1-dimensional original solution in the form of trigonometric series is given by equation 1[32]:

$$\frac{M_t}{M_\infty} = 1 - \sum_{q=0}^{\infty} \frac{8}{(2q+1)^2 * \pi^2} \exp\left[\frac{-D\,(2q+1)^2 * \pi^2}{l^2} t\right] \quad \text{..... (1)}$$

where q is the number of terms, D is the effective diffusivity and t is the time.

Since equation 1 is an infinite series, a typical D value of 10^{-13} m^2/s was used to approximate the number of significant terms. Initial curve fitting to equation 1 revealed negligible differences in WUR predictions beyond 10 terms[1]. Hence, further data analysis was performed with an approximation of the original solution to ten terms. Using least squares error method in MATLAB, experimental WUR values over three months of sample storage at 20 ºC were fitted in this equation and the obtained effective diffusivity values are reported in Table 1.

The effective diffusivities of water in the samples are of the order of 10^{-13} m^2/s which is in agreement with the values reported by Biquet and Labuza for water diffusion in chocolate[1]. However it is worth mentioning that the study by Biquet and Labuza was performed using gravimetric method. Through non-linear curve fitting of data produced by Biquet and Labuza, Antunes and Antunes also obtained D values in the order of 10^{-13} m^2/s at relative humidity 85%[33]. Yuan et al. who studied moisture migration in palm kernel oil by means of gravimetric method reported a D value of 6.02 x 10^{-8} m^2/s at 25 ºC[34]. Their value is a few orders of magnitude higher than the D obtained in the present study. Although the discrepancy between the values obtained for effective diffusivity in different studies can be related to the differences in the food compositions, storage temperature, and the experimental procedure, it is important to consider the usage of the different method of estimations[23]. Moreover, the difference in phase of water migrating through the lipid systems (vapor or liquid phase) contributes to the variation of diffusivity reported in different studies. Yuan et al. highlighted that there is a need to specifically study liquid-induced moisture migration as it is closer to real-world problems and the mechanism is different from vapor-induced migration into lipids[21]. On the other hand, most of the previous studies were done on steady-state permeability values of vapor-induced moisture migration under water activity of 0.85; unlike liquid water used by Yuan et al.[34] and in this study. Furthermore, in comparison to permeability, which describes steady state behavior; the present study reports an unsteady state diffusivity value as a more comprehensive description of moisture migration as a function of time and can be used to solve diffusion equations.

Overall consideration of the results obtained in this study suggests that water migration in all the fat systems is governed by applied processing conditions. As documented in Table 1, dynamically crystallized samples show a lower diffusivity of water than fats crystallized under

the static conditions. Due to the positive correlation between the solid fat content (SFC) and water barrier efficiency of samples[6], their SFC was measured prior to starting the migration process. Martini et al.[35] determined the effect of SFC on water vapor permeability of fat barrier films. They found that as solid fraction in lipids increased, their water vapor permeability decreased. This suggests that moisture permeates more readily through the liquid fraction of lipid compared to the solid crystals. In order to isolate the effect of shearing on moisture diffusion in lipid samples, it was important for us to maintain the same solid fat content in all samples. As reported in Table 1, although the average liquid fraction of the samples varies between samples of different chemical formulations, statistical analysis confirmed the similarity in SFC values of samples with same formulation made under different processing conditions. It is seen that samples processed under different conditions exhibit a marked difference in moisture diffusivities but not in their SFC values indicating the need to examine the underlying mechanism of mass transport. A detailed analysis of the mechanism of moisture migration may better explain the relationship between the samples characteristics and water migration rate.

To fully understand mass transfer of water into lipids, mobility of the penetrant water molecules must be examined relative to the relaxation behavior of lipid matrix. Depending on these relative rates, there are three major categories of mass transport called Case I or Fickian, Non-Fickian or Anomalous, and Case II diffusion[18]. In Case I, the diffusion is slower compared to matrix mobility and therefore acts as the dominating cause of moisture migration. Deviation from this behavior, known as Non-Fickian diffusion, has comparable rates of diffusion and relaxation mechanisms within the matrix. Relaxation mechanisms in the matrix are often associated with physical changes such as swelling or phase transitions[18,36]. An extreme of this deviation is Case II or Super Case II transport, in which diffusion rate is much greater than

matrix relaxation rate and swelling kinetics dominate[18,32]. It is worth mentioning that the obtained effective diffusivity, *D*, accounts for all forms of mass transfer occurring in the system[5].

The mechanism of moisture migration (Fickian, Non-Fickian or Case II) can be determined by using a short-time approximation to original solution of Fick's II law of diffusion. This approximation, known as power law[32] (equation 2) is only valid for water uptake ratio, M_t / $M_\infty < 2/3$:

$$\frac{M_t}{M_\infty} = k\, t^n \qquad \text{.....(2)}$$

Here *k* is the uptake rate parameter and the value of exponent, *n*, is determined by fitting experimental data. The migration mechanism can be determined by comparing exponent *n* with threshold values depending on the geometry of the matrix into which diffusion occurs; planar, cylindrical or spherical. Ritger and Peppas developed semi-empirical equations with different *n* values for drug release from thin polymer slabs, cylinders, spheres, and discs under the perfect sink condition[37]. Their study presented different cut-off *n* values for Fickian diffusion corresponding to each geometry; 0.5 for slabs, 0.45 for cylinders and 0.43 for spheres. Another study by Korsmeyer et al. on diffusional release mechanism determined the threshold values of *n* from cylindrical tablets and reported $n \leq 0.45$ for Fickian, 0.45 to 0.89 for Non-Fickian, 0.89 for Case II transport, and higher than 0.89 for Super Case II transport[38]. Therefore, in this study we assumed an infinite gel source of water to determine the moisture migration into thin lipid layers with slab geometry and considered threshold *n* values for thins slabs *(*$n \leq 0.5$ for Fickian, 0.5 to 1.0 for Non-Fickian, greater than 1 for Case II transport) suggested by Peppas and Brannon-Peppas[32] and Peppas and Sahlin[39]. Experimental data were fitted to equation 2 and the power law exponent (*n*) and uptake parameter (*k*) are reported in Table 2. Since curve fitting analysis required at least two other points besides time 0 (WUR=0), the limitation of WUR< 2/3 on

equation 2 was stretched to values specified in Table 2. The mechanism of moisture migration is described based on the obtained *n*-values reported in this table. For instance, dynamic CB (*n* = 0.5) is described as Fickian diffusion, in which WUR is proportional to $t^{0.5}$ at short times. All other samples exhibit Non-Fickian transport in which rates of diffusion and matrix relaxation are comparable[18].

To describe water uptake in Non-Fickian transport, Alfrey et al. proposed an expression (equation 3) which adds up contributions from diffusion-controlled and relaxation-controlled water uptake[40].

$$\frac{M_t}{M_\infty} = k_1 t^n + k_2 t^{2n} \quad \text{..... (3)}$$

Here exponent *n* for any geometry was defined by aspect ratio of 2*a*/*l* where 2*a* is the diameter and *l* is the thickness; k_1 is the diffusion coefficient and k_2 is the characteristic relaxation constant. These coefficients individually describe Fickian (k_1) and Case II transport (k_2) as follows. Fickian transport is described by a single parameter, the diffusion coefficient, $k_1 = 4\,(D/\pi\, l^2)^{0.5}$, where *D* is constant penetration diffusion coefficient, *l* is slab thickness[32]. Case II transport is described by another single parameter, the characteristic relaxation constant, $k_2 = 2\, k_0/\, C_0\, l$ where k_0 is Case II relaxation constant, C_0 is equilibrium water concentration[32,41]. The generalized equation (3) was later modified by Peppas and Sahlin for thin slabs with *n* = 0.5 (equation 4)[39]. Similar to other short-time approximations (equations 2-3), the following is also valid only for WUR < 2/3:

$$\frac{M_t}{M_\infty} = k_1 t^{0.5} + k_2 t \quad \text{..... (4)}$$

Experimental WUR data were fitted to equation 4 to determine diffusion and relaxation constants in Non-Fickian moisture migration into lipids with thin slab geometry. Model parameters k_1 and

k_2 were determined by least squares fitting and reported in Table 3. The curve-fitted data are plotted in Figure 5 along with experimental WUR data for visual comparison. It is observed that static samples had larger characteristic relaxation constants (k_2) compared to dynamic samples (Table 3). Furthermore, the relative contribution of diffusional (F) and relaxational (R) mechanism can be approximated by fitting a heuristic model containing both phenomena[39]. The contribution ratio is proportional to p^{th} power of time through proportionality constant k_2 / k_1 (equation 5).

$$\frac{R}{F} = \frac{k_2}{k_1} t^p \quad \text{.....(5)}$$

Based on k_1 and k_2 values, the proportionality constant, k_2 / k_1 is calculated and reported in Table 3. This ratio k_2 / k_1 ranges from 0 to 1 indicating a shift from pure Fickian diffusion-controlled to relaxation-controlled mechanism of water uptake. For dynamic CB, the ratio k_2 / k_1 is 0 indicating that moisture migration occurs solely through Fickian diffusion. In all other samples, this ratio is greater than 0 suggesting that the contribution of relaxation mechanism in moisture migration is not negligible and should be taken into consideration. In static CB, the relative contribution of relaxation mechanism to Fickian diffusion is about 27% ($k_2 / k_1 = 0.27$). In PO, static samples have a higher ratio of k_2 / k_1 (0.13) compared to dynamic samples with k_2 / k_1 of approximately 0.08. Based on this result, two conclusions can be made: (i) Relaxation of matrix has a larger contribution in static samples compared to sheared samples suggesting that rate of relaxation is affected by the structure of the matrix. (ii) The dynamics of moisture migration is a function of lipids' chemical compositions as sheared PO and sheared CB showed different mechanism of moisture diffusivity. This finding could be highlighted more by considering the results obtained from the binary mixture of palm kernel oil and cocoa butter. In the case of CPPO, dynamic samples did not reach the equilibrium (Figure 2 (c)) during the

storage time of this study and mass transfer mechanism could not be modeled using equations 1-5. A high ratio of k_2 / k_1 (about 0.64) was obtained in the statically crystallized CPPO, indicating that relaxation mechanism is dominating in these samples. Interestingly the non-sheared CPPO samples showed the highest contribution of the relaxation mechanism (~64%) among all the lipid systems examined in this study. This prominent relaxation rate could be due to significant swelling stresses or phase changes of the matrix due to the presence of cocoa powder. Ghosh et al. found that during moisture permeability tests, cocoa powder particles swell and change the structure of the matrix[42]. Svanberg et al. also reported rapid swelling of chocolate exposed to water activity of 0.8 or higher[43]. Therefore, in cocoa powder containing lipid mixtures, it is expected to see a greater contribution of matrix relaxation and swelling induced by moisture uptake. The sheared CPPO samples had slower migration compared to all other samples and did not reach equilibrium during the storage period of this study. Although one may suggest that the slow moisture uptake of sheared CPPO could be attributed to the additive effect of shearing found through this study and also the swelling effect of cocoa powder particles studied by Ghosh et al.[42], a detailed study and analysis of this set of samples is proposed by the authors.

Conclusions

Moisture migration occurred in all lipid samples stored at 20 ^{0}C and experimental data showed that effective diffusivity of water in lipids is a function of system composition and the applied crystallization process. Shearing was found to decrease diffusion and increase moisture barrier properties of the lipid systems, when a higher water migration rate was obtained in the statically crystallized samples.

It was also observed that moisture migration occurred through a combination of two phenomena, Fickian diffusion and relaxation of the matrix. This combination, known as Non-Fickian or

anomalous diffusion, occurred in all tested lipids samples except dynamically crystallized cocoa butter which displayed pure Fickian diffusion. Although Fickian diffusion was found to be dominant over relaxation mechanism in palm kernel oil samples, relaxation of CPPO matrix created by mixing cocoa powder in palm kernel oil is found to be rate controlling phenomena for moisture migration in the CPPO samples. In order to fully understand the exact mechanism of water permeability, further study is required to consider the effect of the fat structures, and the direct correlation between the micro/nano structural properties and the mechanisms of mass transportation.

Acknowledgements

The authors would like to thank the Center for Advanced Processing and Packaging Studies at The Ohio State University for providing partial funding for this research. We also wish to thank Dr. Amir Abduljalil at the Department of Radiology, The Ohio State University, for his expert assistance in conducting MRI experiments and generating data.

References

1 B. Biquet and T. P. Labuza, *J. Food Sci.,* 1988, **3** (4), 989-998.

2 V. Guillard, B. Broyart, C. Bonazzi, S. Guibert and N. Gontard, *J. Food Sci.,* 2003, **68** (3), 958-966.

3 S. Martini, D.A. Kim, M. Ollivon and A. G. Marangoni, *J. Agric. Food Chem.,* 2006, **54**, 1880-1886.

4 T. P. Labuza and C. R. Hyman, *Trends Food Sci. Tech.,* 1998, **9** (2), 47-55.

5 J. M. Aguilera, M. Michel, and G. Mayor, *J. Food Sci*., 2004, **69** (7), 167–174.

6 V. Morillon, F. Debeaufort, G. Blond, M. Capelle and A. Voilley, *Crit. Rev. Food Sci. Nutr*., 2002, **42** (1), 67-89.

7 G. V. Barbosa-Canovas, A. J. Jr. Fontana, S. J. Schmidt and T. J. Labuza, *Water activity in foods: Fundamentals and applications*, IFT Press, Blackwell Publishing, Ames, Iowa, 2007.

8 J. J. Kester and O. Fennema, *J Food Sci.,* 1989, **54**, 1383-1389.

9 M. Martin-Polo, A. Voilley, G. Blond, B. Colas, M. Mesnier and N. Floquet, *J. Agric. Food Chem*., 1992, **40**, 413–418.

10 H. Grigoriew and A. G. Chmielewski, *J. Mater. Sci. Lett.,* 1997, **16**, 1945–1947.

11 D. Dhonsi and A. G. F. Stapley, *J. Food Eng.,* 2006, **77** (4), 936–942.

12 S. Sonwai and M. R. Mackley, *J. Am. Oil Chem. Soc.,* 2006, **83** (7)*,* 583–596.

13 F. Maleky and A. G. Marangoni, *Cryst. Growth Des*., 2011, **11***,* 2429–2437.

14 R. Campos and A. G. Marangoni, *Cryst. Growth Des.,* 2014, **14** (3), 1199–1210.

15 J. Foley and J. P. Brady, *J. Dairy Res.,* 1984. **51**, 579-589.

16 F. Maleky and A. G. Marangoni, *Soft Matter,* 2011, **7**, 6012-6024.

17 F. Maleky, K. L. McCarthy, M. J. McCarthy and A. G. Marangoni, *J. Food Sci.,* 2012, **77** (3), 74-79.

18 V. Ghosh, G. R. Ziegler and R. C. Anantheswaran, *CRC Reviews in Food Sci. & Nutrition,* 2002, **42** (6), 583-626.

19 T. H. McHugh and J. M. Krochta, *J. Food Process. Preserv.,* 1994, **18***,* 173-188.

20 M. B. Perez-Gago and J. M. Krochta, *J. Agric. Food Chem*., 2001, **49***,* 9996-1002.

21 Q. Yuan, W. Hanselmann and R. C. Anantheswaran, *J. Food Eng.,* 2009, **95***,* 460-470.

22 A. Fabbri, C. Cevoli and R. Troncoso, *Food Res. Int.,* 2014, **56***,* 63–67.

23 H. Watanabe and M. Fukuoka, *Trends Food Sci. Tech*., 1992, **3**, 211-215.

24 P. Cornillon and L. C. Salim, *Magn. Reson. Imaging,* 2000, **18***,* 335–41.

25 Y. J. Choi, K. L. McCarthy, M. J. McCarthy and M. H. Kim, *Appl. Magn. Reson.,* 2007, **32**, 205–220.

26 K. L. McCarthy and M. J. McCarthy, *J. Food Sci.,* 2008, **73** (6), 266–273.

27 A. Lodi, A. M. Abduljalil and Y. Vodovotz, *Magn. Reson. Imaging,* 2007, **25**, 1449–1458.

28 M. Y. Troutman, I. V. Mastikhin, B. J. Balcom, T. M. Eads and G. R. Ziegler, *J. Food Eng.,* 2001, **48**, 257–267.

29 W. L. Lee, M. J. McCarthy and K.L. McCarthy, *J. Food Sci.,* 2010, **75** (1), E83-89.

30 A. Altan, D. M. Lavenson, M. J. McCarthy and K. L. McCarthy, *J. Food Sci.,* 2011, **76** (6), E489- 494.

31 J. Crank, *Mathematics of Diffusion,* Claredon Press, Oxford, England, 1975.

32 N. A. Peppas and L. Brannon-Peppas, *J. Food Eng*., 1994, **22***,* 189–210.

33 A. C. B. Antunes and L. J. Antunes, *Int J. Food Sci. Tech.,* 2000, **35**, 323-329.

34 Q. Yuan, W. Hanselmann and R. C. Anantheswaran, *J. Food Eng*., 2012, **108**, 13-21.

35 S. Martini, D. A. Kim, M. Ollivon and A. G. Marangoni, *Food Res. Int.,* 2006, **39***,* 550-558.

36 I. A. Taub and R. P. Singh, *Food Storage Stability,* CRC Press, Inc., Bacon Raton, Florida, 1998.

37 P. L. Ritger and N. A. Peppas, *J. Control Release,* 1987, **5**, 23-26.

38 R. W. Korsmeyer, R. Gurny, E. Doelker, P. Buri and N. A. Peppas, *Int J. Pharm.,* 1983, **15**, 25-35.

39 N. A. Peppas and J. J. Sahlin, *Int. J. Pharm.,* 1989, **57***,* 169-172.

40 T. Alfrey, E. F. Gurnee and W. G. Lloyd, *J. Polym Sci*., 1966, **12** (1), 249-261.

41 D. J. Enscore, H. B. Hopfenberg and V. T. Stannett, *Polym. Eng. Sci.,* 1980, **20** (1)*,* 102-107.

42 V. Ghosh, G. R. Ziegler and R. C. Anantheswaran, *J. Food Eng.,* 2005, **66** (2), 177-186.

43 L. Svanberg, N. Loren and L. Ahrne, *J. Food Sci*., 2012, **77** (11), 328-334.

Tables:

Table 1. Solid fat contents (SFC) and effective diffusivities (D) of the samples at a storage temperature of 20 ºC for three months

Sample	Dynamic			Static		
	SFC (%)	D x 10^{13} (m^2/s)	least squares error	SFC (%)	D x 10^{13} (m^2/s)	least squares error
Cocoa butter	80.2	2.41	0.09	81.3	4.87	0.07
Palm kernel oil	70.4	3.61	0.17	69.8	5.43	0.04
Cocoa Powder in Palm kernel oil	59.4	ND*	ND	60.8	4.86	0.02

** ND stands for not determined.*

Note- All values are calculated from original solution to Fick's II law of diffusion.

Table 2. Nonlinear curve fitting for power law exponent determine water migration mechanism in the lipid systems

Sample	Dynamic			Static		
	WUR	k	n	WUR	k	n
Cocoa butter	<0.63	0.14	0.51	<0.77	0.13	0.71
Palm kernel oil	<0.79	0.12	0.63	<0.73	0.14	0.65
Cocoa Powder in Palm kernel oil	ND*	ND	ND	<0.75	0.09	0.78

** ND stands for not determined.*

Note- In the above table, k is the uptake parameter and n is the power law exponent which describes Fickian (n = 0.5), Non-Fickian (0.5< n <1), or Case II transport (n = 1).

Table 3. Nonlinear curve fitting to determine relative contributions of Fickian and relaxation mechanism in transport of water in the lipid systems

Sample	Dynamic				Static			
	k_1 ($day^{-0.5}$)	k_2 (day^{-1})	R^2	k_2 / k_1	k_1 ($day^{-0.5}$)	k_2 (day^{-1})	R^2	k_2 / k_1
Cocoa Butter	0.14	0	0.94	0	0.11	0.03	0.96	0.27
Palm kernel oil	0.13	0.01	0.96	0.08	0.14	0.02	0.95	0.13
Cocoa Powder in Palm kernel oil	ND*	ND	ND	ND	0.06	0.04	0.98	0.64

** ND stands for not determined.*

Figure Captions:

Figure 1 (a) Schematic 3-D image of samples (6 cm in height and with 3 cm square ends) with lipid layer on the top of the gel. (b) MR Image of sample immediately after preparation (t=0). Axes represent pixel numbers (0 to 200). (c) 1-D SI profile of the sample on day 1 and 91 of storage at 20 ºC.

Figure 2 - Moisture uptake values in arbitrary units (a.u.) for lipid samples over three months of storage at 20 ºC, (a) cocoa butter, (b) palm kernel oil, (c) cocoa powder in palm kernel oil. Solid squares represent static samples and triangles represent dynamic samples.

Figure 3 - Moisture uptake values in arbitrary units (a.u.) for lipid samples at 7 days (striped bars) and 91 days (grey bars) of storage at 20 °C, (a) cocoa butter (CB), (b) palm kernel oil (PO), (c) cocoa powder in palm kernel oil (CPPO). The symbols indicate statistical differences between two time points of the same sample with α=0.05.

Figure 4 - Moisture uptake values in arbitrary units (a.u.) for lipid samples prepared with dynamic (dotted bars) and static crystallization (black bars) after 61 days of storage at 20° C. The symbols indicate statistical differences between two methods of crystallization of the same lipid with α=0.05.

Figure 5 - Water uptake ratio for lipid samples over three months of storage at 20 ºC, (a) cocoa butter, (b) palm kernel oil, (c) cocoa powder in palm kernel oil. Solid squares represent static samples and triangles represent dynamic samples. Filled markers represent experimental data and hollow markers represent curve fitted data described by equation 4 with parameter values in table 3.

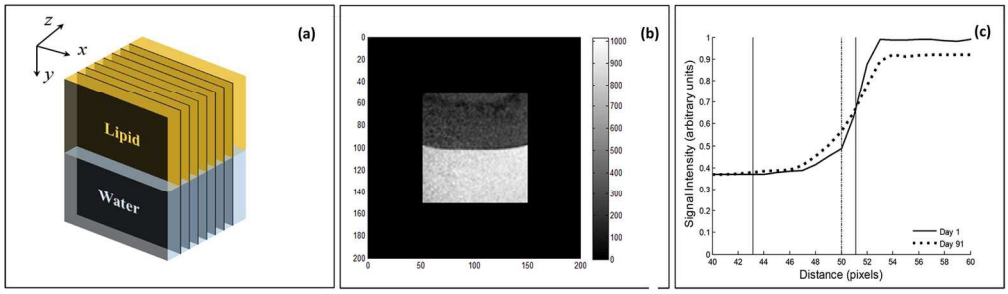

Figure 1 (a) Schematic 3-D image of samples (6 cm in height and with 3 cm square ends) with lipid layer on the top of the gel. (b) MR Image of sample immediately after preparation (t=0). Axes represent pixel numbers (0 to 200). (c) 1-D SI profile of the sample on day 1 and 91 of storage at 20 ºC.
150x44mm (300 x 300 DPI)

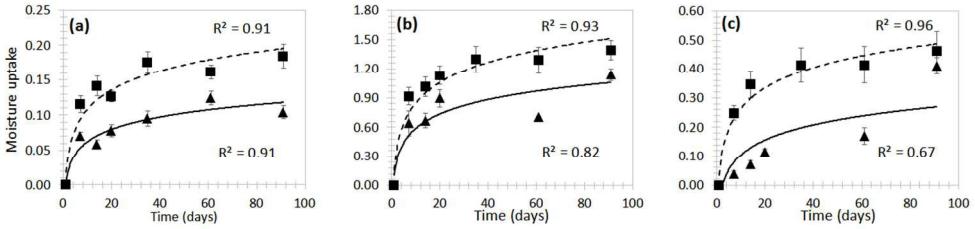

Figure 2 - Moisture uptake values for lipid samples over three months of storage at 20 ºC, (a) cocoa butter, (b) palm kernel oil, (c) cocoa powder in palm kernel oil. Solid squares represent static samples and triangles represent dynamic samples.

112x28mm (300 x 300 DPI)

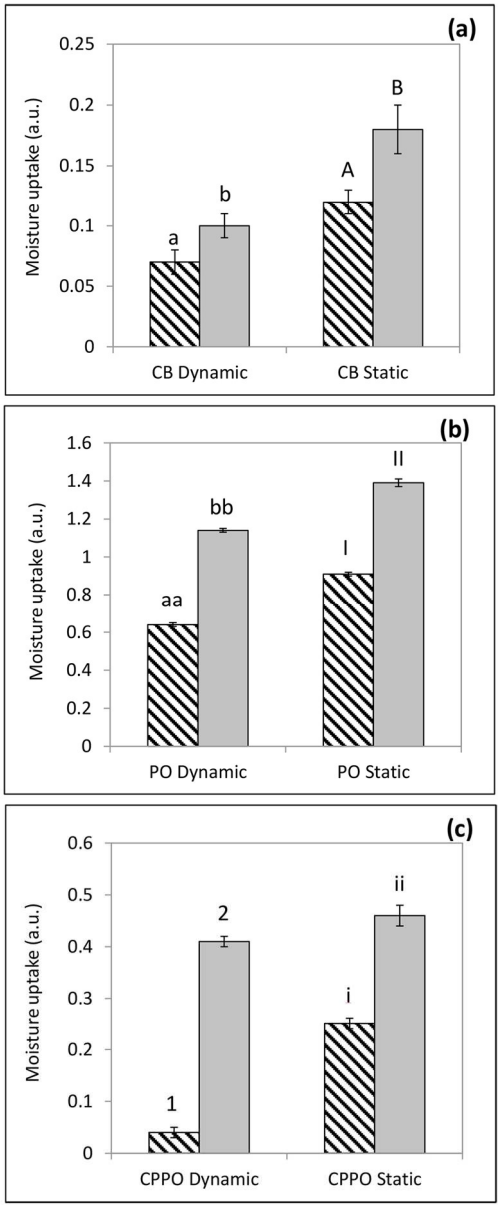

Figure 3 - Moisture uptake values in arbitrary units (a.u.) for lipid samples at 7 days (striped bars) and 91 days (grey bars) of storage at 20 °C, (a) cocoa butter (CB), (b) palm kernel oil (PO), (c) cocoa powder in palm kernel oil (CPPO). The symbols indicate statistical differences between two time points of the same sample with α=0.05.
80x189mm (300 x 300 DPI)

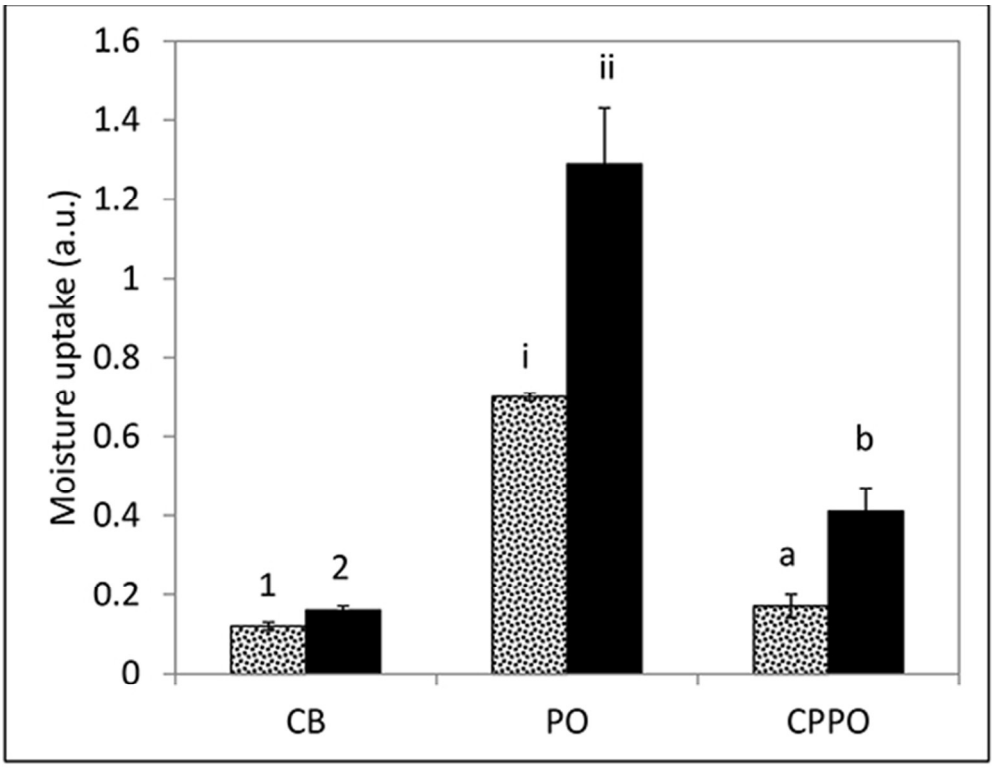

Figure 4 - Moisture uptake values in arbitrary units (a.u.) for lipid samples prepared with dynamic (dotted bars) and static crystallization (black bars) after 61 days of storage at 20° C. The symbols indicate statistical differences between two methods of crystallization of the same lipid with α=0.05.
50x38mm (300 x 300 DPI)

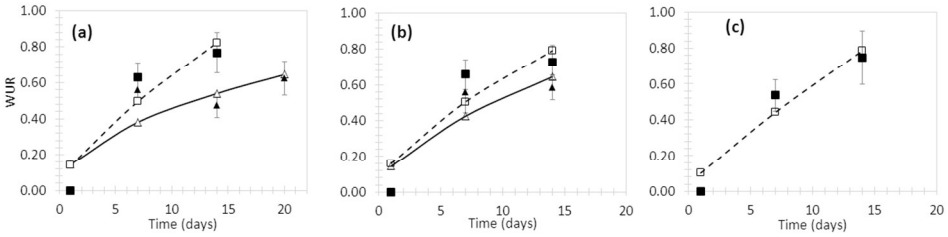

Figure 5 - Water uptake ratio for lipid samples over three months of storage at 20 ºC, (a) cocoa butter, (b) palm kernel oil, (c) cocoa powder in palm kernel oil. Solid squares represent static samples and triangles represent dynamic samples. Filled markers represent experimental data and hollow markers represent curve fitted data described by equation 4 with parameter values in table 3.
109x30mm (300 x 300 DPI)